Supplementary information

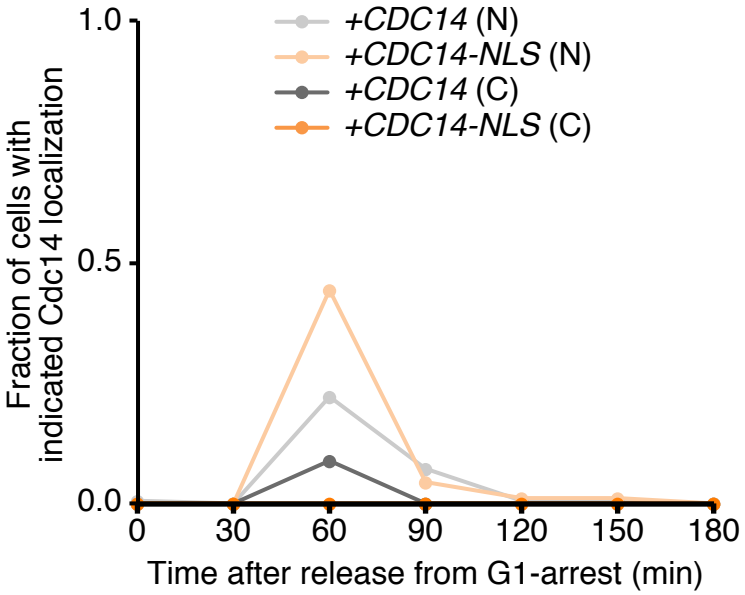
1.0
0.5
0.0
Fraction of cells with indicated Cdc14 localization
+CDC14 (N)
+CDC14-NLS (N)
+CDC14 (C)
+CDC14-NLS (C)
0
30
60
90
120
150
180
Time after release from G1-arrest (min)

FIGURE S1

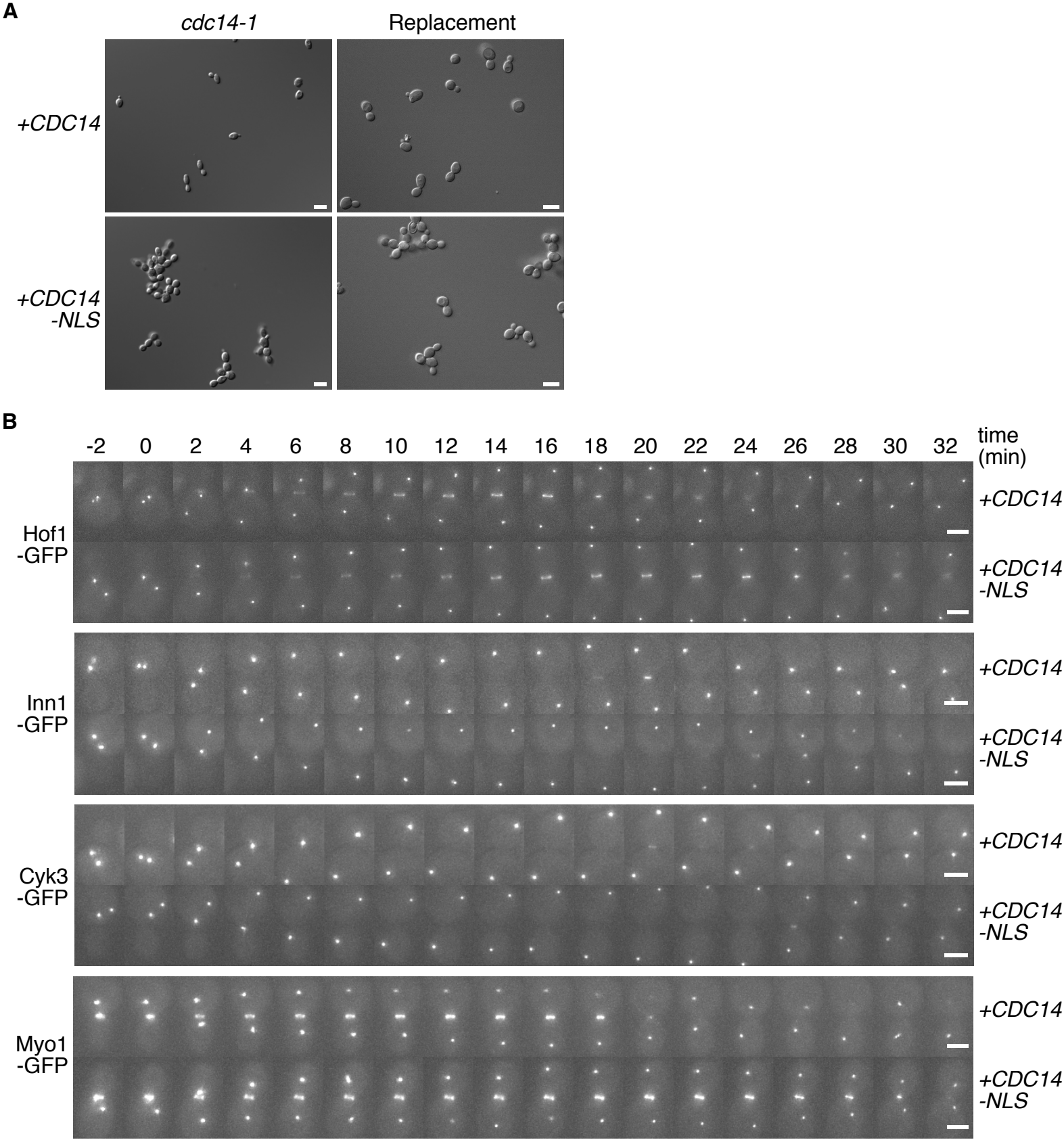
A
cdc14-1
Replacement
+CDC14
+CDC14
-NLS
B
-2
0
2
4
6
8
10
12
14
16
18
20
22
24
26
28
30
32
time
(min)
Hof1
-GFP
Inn1
-GFP
Cyk3
-GFP
Myo1
-GFP
+CDC14
+CDC14
-NLS
C
Parental
Parental
cyk3Δ
cdc14-3
Parental
hof1Δ
+CDC14
+CDC14-NLS
+CDC14
cyk3Δ
+CDC14-NLS
cyk3Δ
+CDC14
hof1Δ
+CDC14-NLS
hof1Δ

FIGURE S2

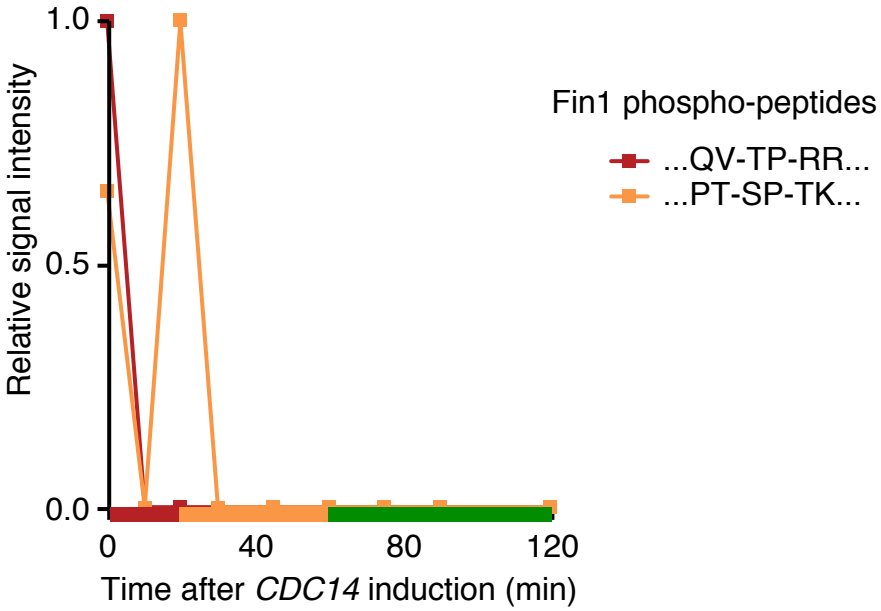
1.0
0.5
0.0
Relative signal intensity
0
40
80
120
Time after *CDC14* induction (min)
Fin1 phospho-peptides
...QV-TP-RR...
...PT-SP-TK...

FIGURE S3

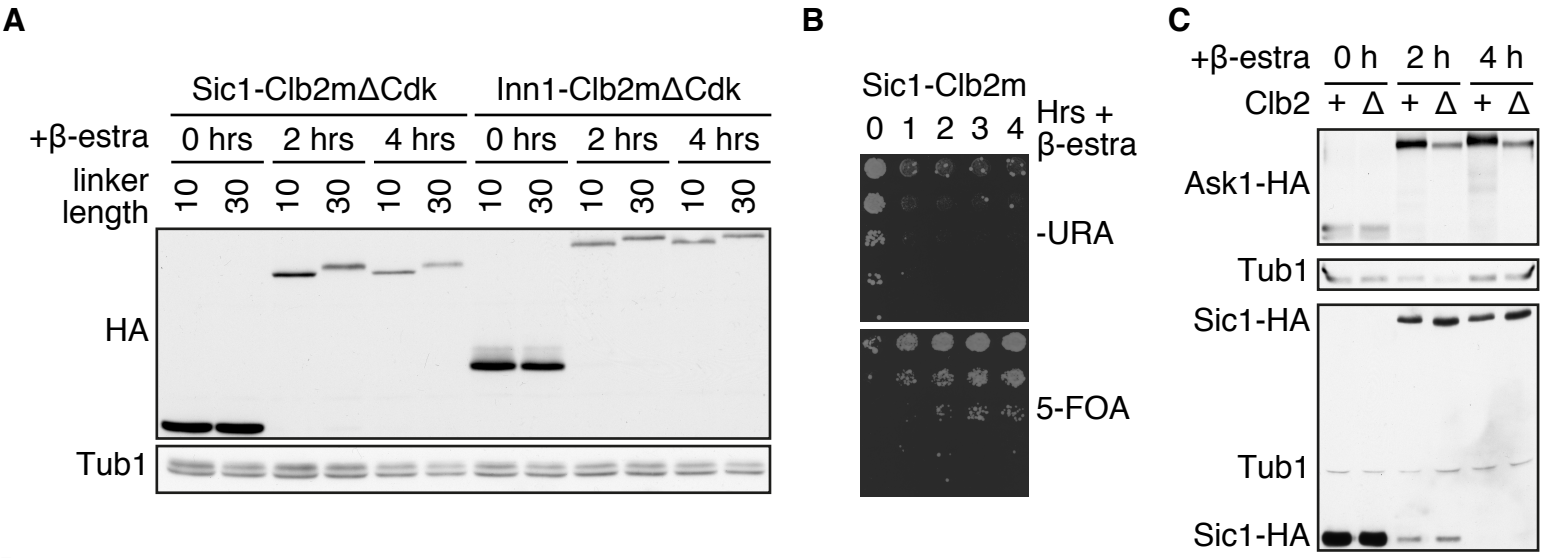

D

Gene	Reason	Cat	Ref	Gene	Reason	Cat	Ref	Gene	Reason	Cat	Ref
Aip1	Act depol		4	Ede1	Screen	2I	3	Kel1	Interactor		2
Bni1	Screen	2L	2	Dma2	Interactor		2	Lsb3	Screen	1I1L	
Bnr1	Interactor		2	Fir1	Screen	1I2L		Nba1	Screen	1L	
Boi1	Interactor		1	Gin4	Screen	1L		Sec3	Screen	1I	
Boi2	Screen	3I		Hof1	Screen	1L		Shs1	Screen	1L	
Bud3	Interactor		2	Hsl1	Interactor		2	Spa2	Screen	7L	
Cdc3	Screen	1L		Inn1	Screen	1I		Ssd3	Screen	1I3L	
Chs2	Screen	6L		Iqg1	Screen	1I1L		Srv2	Act depol		4
Crn1	Interactor		3	Kcc4	Interactor		1				

1) Breitkreutz et al., 2010; 2) Bloom et al., 2011; 3) Own immunoprecipitation-mass spectrometric identification (data not shown); 4) Moseley and Goode, 2006

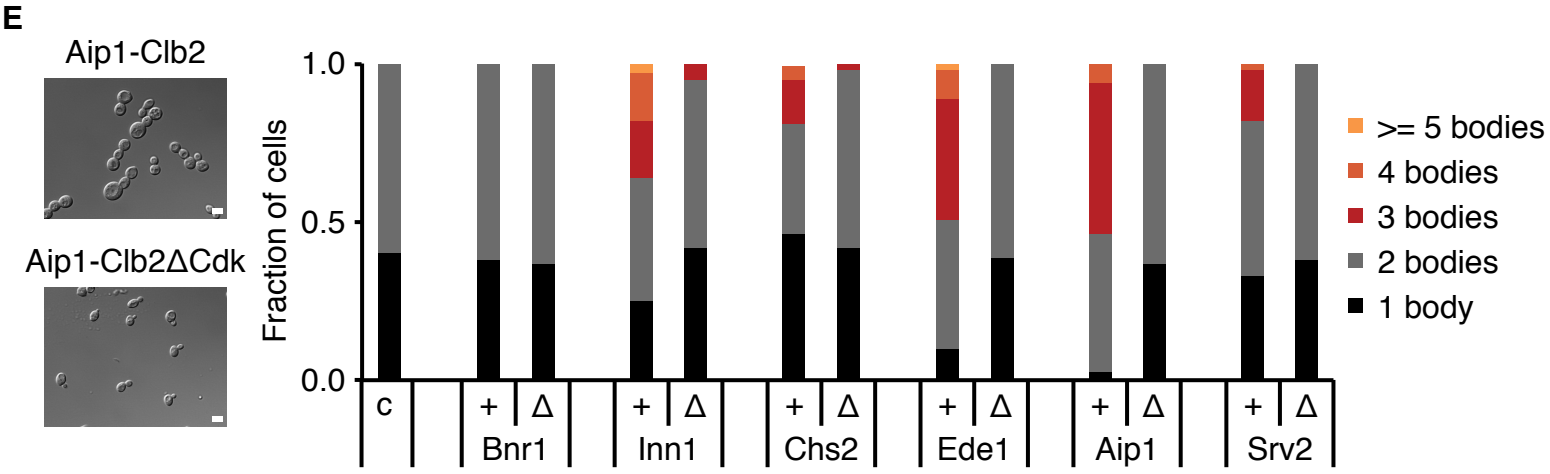

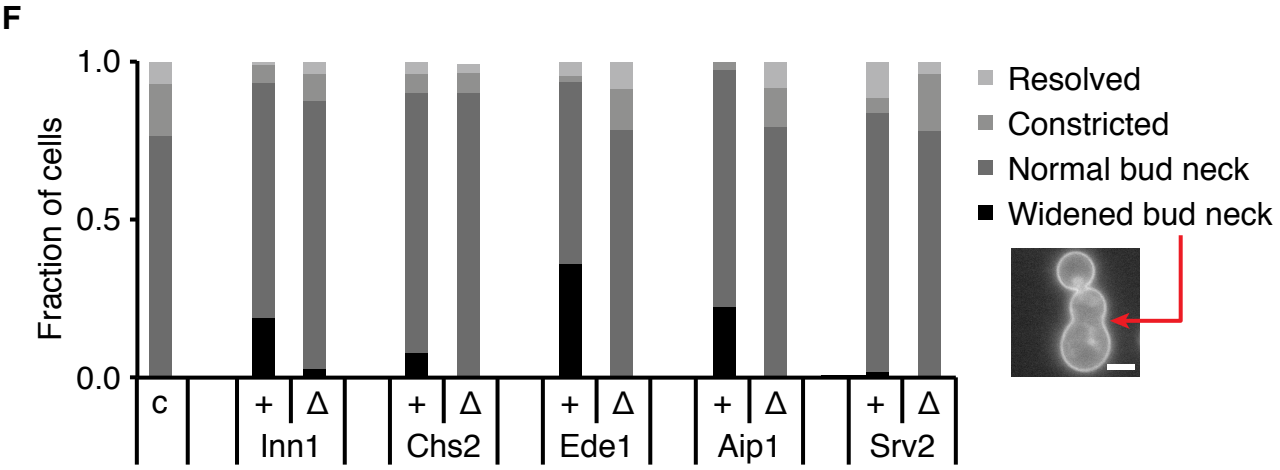

FIGURE S4

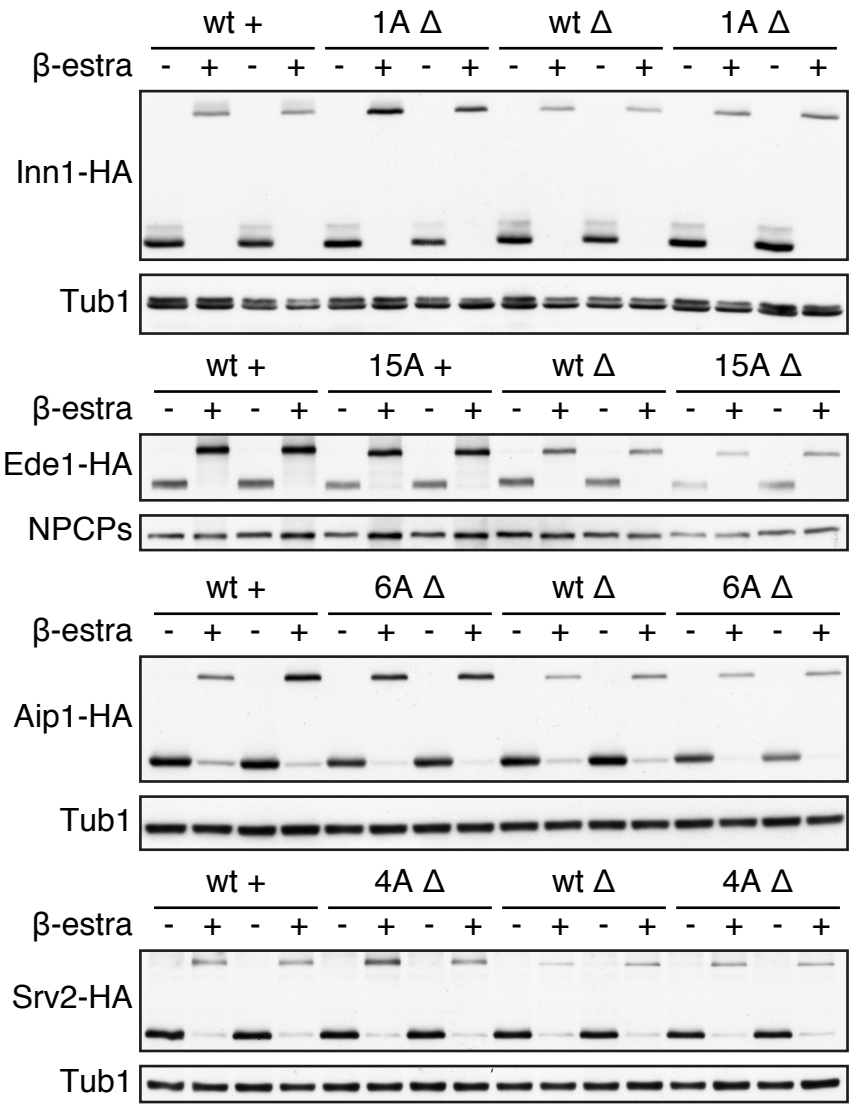
wt +
1A Δ
wt Δ
1A Δ
β-estra
- + - + - + - + - + - + - + - +
Inn1-HA
Tub1
wt +
15A +
wt Δ
15A Δ
β-estra
- + - + - + - + - + - + - + - +
Ede1-HA
NPCPs
wt +
6A Δ
wt Δ
6A Δ
β-estra
- + - + - + - + - + - + - + - +
Aip1-HA
Tub1
wt +
4A Δ
wt Δ
4A Δ
β-estra
- + - + - + - + - + - + - + - +
Srv2-HA
Tub1

FIGURE S5

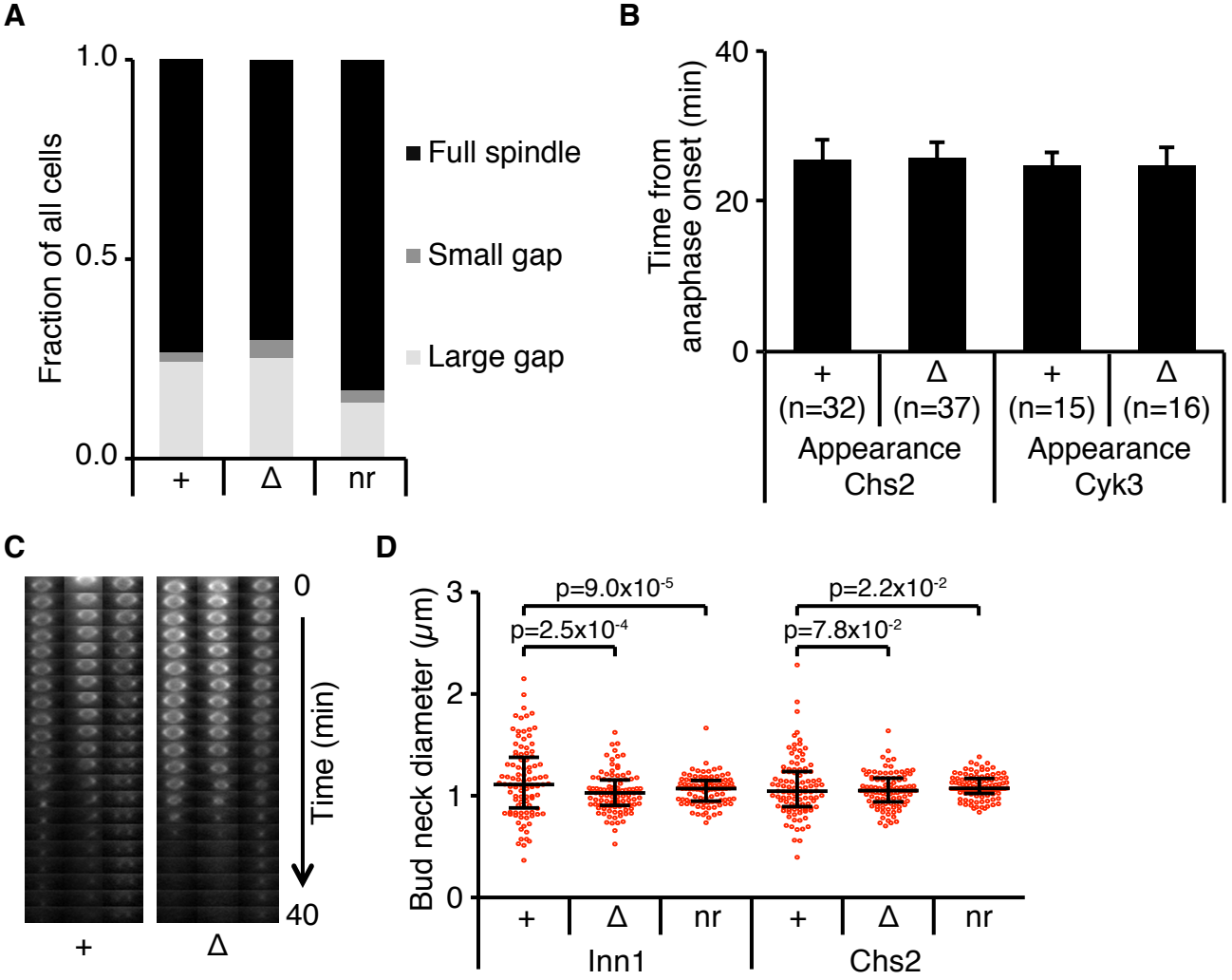
A
1.0
0.5
0.0
Fraction of all cells
Full spindle
Small gap
Large gap
+
Δ
nr
B
40
20
0
Time from anaphase onset (min)
+ (n=32)
Δ (n=37)
+ (n=15)
Δ (n=16)
Appearance Chs2
Appearance Cyk3
C
0
Time (min)
40
+
Δ
D
p=9.0x10-5
p=2.5x10-4
p=2.2x10-2
p=7.8x10-2
Bud neck diameter (μm)
3
2
1
0
+
Δ
nr
+
Δ
nr
Inn1
Chs2

FIGURE S6

Supplementary figure legends

Supplementary Figure S1 Cdc14-NLS is constrained to the nucleus. +*CDC14* and +*CDC14-NLS* cells were released from α-factor-induced synchronization in G1 to pass through the cell cycle, and arrested again in the next G1 phase by re-addition of α-factor. Cdc14 localization as observed in Figure 1A was scored as nucleolar/nuclear (N) or cytoplasmic (C), and the quantification over time is shown (n>100). This analysis confirms that Cdc14-NLS remained constrained to the nucleus and did not reach cytoplasmic accumulation at any time.

Supplementary Figure S2 Characterization of +*CDC14-NLS* cells. (**A**) +*CDC14* or +*CDC14-NLS* cells, either in the *cdc14-1* background or as a replacement of the endogenous *CDC14* allele, were grown at the 35.5ºC for 5 h, sonicated and photographed. While +*CDC14* cells display the normal budding yeast morphology, +*CDC14-NLS* cells grow as large aggregates. This confirms that cytoplasmic Cdc14 is required for cytokinesis, but not for other aspects of cell cycle progression. Scale bars, 10 µm. (**B**) Still images of example movies that were used for the timing of cytokinesis events in Figure 2E. Time point 0 is defined as the last frame when the spindle pole bodies do not yet display anaphase movement. Scale bars, 5 µm. (**C**) Parental, +*CDC14* and +*CDC14-NLS* cells with or without *hof1Δ* or *cyk3Δ* were grown at 34ºC for 2 days. The synthetic growth defect of +*CDC14-NLS* cells with *hof1Δ*, but not *cyk3Δ*, argues for a role of Cdc14 in a cytokinesis pathway parallel to Hof1 and possibly related to the role of Cyk3.

Supplementary Figure S3. Disappearance of Fin1 phospho-peptides. The abundance of the two Fin1 phospho-peptides detected in our phospho-proteome are shown during Cdc14-induced mitotic exit.

Supplementary Figure S4. Screen for phospho-regulated cytokinesis factors. (**A**) As part of optimizing the gene targeting strategy to fuse Clb2m to candidate cytokinesis regulators, we compared the influence of the length of a flexible linker between the target protein and Clb2m on the stability of the resulting fusion protein. Shown is a time course of β-estradiol treatment to

induce recombination of a Clb2mΔCdk fusion with a linker length of 10 or 30 amino acids with Sic1 or Inn1. Western blotting confirms comparable recombination efficiencies and protein stability after recombination with either linker length. Therefore a linker length of 30 amino acids, aimed at facilitating kinase access also to remote domains of to the protein of interest, was used for the subsequent screening of potential cytokinesis regulators. (**B**) Assay to evaluate recombination efficiency following β-estradiol treatment. Serial dilutions of a culture of Sic1-Clb2m cells at the indicated times after β-estradiol addition were spotted on medium lacking uracil and on 5-fluoro orotic acid (5-FOA) containing medium. Cre recombinase-mediated fusion of Sic1 with Clb2m results in removal of the *URA3* auxotrophic marker gene. Recombination appears to be complete within 1-2 hours, based on the loss of growth on medium lacking uracil and the acquired resistance to 5-FOA. (**C**) Ask1 (upper panels) and Sic1 (lower panels) were conditionally fused to Clb2m (+) or Clb2mΔCdk (Δ), and cell lysates were subjected to Western blotting analysis. For both proteins, a large electrophoretic mobility shift caused by the cyclin fusion is apparent within 2 hours of β-estradiol treatment. In addition, Ask1 and Sic1 fused to Clb2m migrated slower compared to fusion with Clb2mΔCdk, consistent with gel retardation due to phosphorylation. Moreover, Sic1-Clb2m levels were lower than Sic1-Clb2mΔCdk levels, as would be expected due to Sic1 destabilization by phosphorylation (Verma *et al*, 1997). Tub1 served as a loading control. (**D**) Overview of the 26 genes in the screen for cytokinetic defects induced by Clb2m fusion. Most genes were included because we found their corresponding phospho-peptides in our mass spectrometry screen (Screen), and they disappeared with intermediate or late timing. The number of detected phospho-peptides and their category (Cat: I, intermediate; L, late) for each protein is indicated. In addition we included proteins that have been described to interact with Cdc14 in the literature (Interactor), with the respective reference given. Finally, we also included three proteins implicated in actin depolymerization (Act depol), two of which are know Cdk substrates, which hold key potential as cytokinesis regulators (Moseley & Goode, 2006). (**E**) Cell chain formation of cells containing Inn1, Chs2, Ede1, Aip1 or Srv2-Clb2m fusions. DIC images were acquired of the cells in Figure 5C (n>100), 6

hours after β-estradiol addition. The number of cell bodies that remained connected after sonication was quantified. In all cases, chains of more than 2 cell bodies were observed upon Clb2m fusion, suggestive of a cytokinesis defect. Cells containing a Bnr1-Clb2m fusion do not display any obvious cytokinesis defects, and were included together with control (c) cells for comparison. Scale bars, 10 µm. (**F**) The phenotypes of all bud necks in cells from Figure 5E were scored into the categories described in Figure 2C (n>100). We included one phenotype in this analysis, i.e., widened bud neck, which is not observed in wild-type cells. An example of a cell in this category is depicted next to the bar graph. Scale bars, 10 µm.

Supplementary Figure S5 Rescue of the Clb2m fusion phenotype by non-phosphorylatable proteins. Western blot analysis of the experiment in Figure 6A, before and 5 hours after addition of β-estradiol. 2 clones for each genotype are shown that were analysed in parallel. This analysis confirms comparable expression levels and recombination efficiencies of the wild type and phospho-site mutant Clb2m fusions.

Supplementary Figure S6 Inn1 phosphorylation regulates bud neck localization and Chs2 activation. (**A**) As Figure 7B, but the overall distribution of spindle phenotypes of all analysed cells (n>250) is compared. This shows that Inn1-Clb2m fusion does not alter the relative abundance or duration of spindle morphologies during mitotic exit. (**B**) The time from anaphase onset to the first detectable appearance at the bud neck of Chs2 or Cyk3, respectively, was determined in Inn1-Clb2m and Inn1-Clb2mΔCdk cells. The experiment was performed as in Figure 2E, but cells were treated with β-estradiol 1 hour prior to start of α-factor synchronization. Despite the severe cytokinesis defects in Inn1-Clb2m cells, bud neck recruitment of Chs2 and Cyk3 occurred with normal kinetics. Error bars represent standard deviations. (**C**) Side projections of actomyosin rings at the time of cytokinesis in Inn1-Clb2m and Inn1-Clb2mΔCdk cells. These examples, included in the quantification in Figure 7F, confirm the penetrance of the ring disintegration phenotype in Inn1-Clb2m cells. (**D**) Bud neck diameters, measured using the GFP-Spo20$^{51-91}$ marker, in asynchronous Inn1/Chs2-Clb2m (+) and Inn1/Chs2-Clb2mΔCdk (Δ)

cells (n=100) 6 h after β-estradiol treatment. Inn1/Chs2-Clb2mΔCdk cells before treatment (non-recombined, nr) were included for comparison. Error bars represent standard deviations.

Supplementary Materials & Methods

Harvesting of yeast cells and digestion of proteins for mass spectrometric analysis

Trichloroacetic acid (at a final concentration 6%) was added to 100 ml of yeast cultures, which were then placed overnight on ice. The yeast cells were pelleted by centrifugation at 1,500xg, the supernatant was discarded, and the cells were resuspended in ice-cold acetone and washed twice. The supernatant was discarded, and the pellet was frozen at -80°C until required for further processing. The yeast cells were lysed by beating with glass beads in 8 M urea, 100 mM ammonium bicarbonate, and 5 mM EDTA. Debris was removed by centrifugation at 16,000g for 10 min. Protein concentration was determined with a BCA protein assay kit (Pierce). Then, for each replicate, 3 mg of total protein was reduced with TCEP (Thermo Scientific) at a final concentration of 10 mM at room temperature for 1 hour. Free thiols were alkylated with 10 mM iodoacetamide at room temperature for 30 min in the dark. The solution was subsequently diluted with 50 mM ammonium bicarbonate (AMBIC) (pH 8.3) to a final concentration of 1.0 M urea, and digested overnight at 37°C with sequencing-grade modified trypsin (Promega) at a protein-to-enzyme ratio of 50:1. Peptides were desalted on a C18 Sepr-Pak cartridge (Waters) and dried under vacuum. The peptides samples were reconstituted in 2% acetonitrile, 0.1% formic acid and analysed by mass spectrometry. Phospho-peptides were isolated using TiO_2 beads as previously described (Bodenmiller & Aebersold, 2010).

Mass spectrometric analysis of peptide samples

Chromatographic separation of peptides was carried out with an Eksigent (Eksigent Technologies) and Proxeon (Proxeon Biosystems) NanoLC system connected to a 15-cm fused-silica emitter with 75-µm inner diameter (BGB Analytik) packed in-house with a Magic C18 AQ 3-µm resin (Michrom BioResources). The phospho-peptide samples were analysed by LC-tandem MS (LC-MS/MS) run with a linear gradient ranging from 95% solvent A (98% water, 2% acetonitrile, 0.1% formic acid) to 35% solvent B (98% acetonitrile,

2% water, 0.1% formic acid) over 90 min at a flow rate of 300 nl/min. Mass spectrometric analysis was performed with a LTQ FT mass spectrometer (Thermo Scientific) equipped with a nanoelectrospray ion source (Thermo Scientific). Mass spectra were acquired in a data-dependent manner, with an automatic switch between MS and MS/MS scans. High-resolution MS scans were acquired in the ICR cell (60,000 FWHM, target value 10^6) to monitor peptide ions in the mass range of 400–1,600 m/z, followed by collision-induced dissociation MS/MS scans in the ion trap (minimum signal threshold 150, target value 10^4, isolation width 2 m/z) of the five most intense precursor ions. The precursor ion masses of scanned ions were dynamically excluded from MS/MS analysis for 10 s. Singly charged ions and ions with unassigned charge states were excluded from triggering MS2 events.

Database search

Raw data were converted to the open mzXML format with ReAdW (version 4.3.1). mzXML files were searched by SEQUEST via Sorcerer Software 4.2.0 and against SGD protein databases (release 07/2010) concatenated with reverse sequences. For *in silico* digestion, trypsin was used as the protease and was assumed to cleave after lysine (K) and arginine (R) unless followed by proline (P). Two missed cleavage sites and one non-tryptic terminus were allowed per peptide. The precursor ion tolerance was set to 50 parts per million (ppm), and fragment ion tolerance was set to 0.5 Dalton. The data were searched allowing phosphorylation (+79.9663 Daltons) of serine, threonine, and tyrosine as a variable modification and carboxy-amidomethylation of cysteine (+57.0214 Daltons) residues as a fixed modification. Finally, the identification results were statistically analysed with the PeptideProphet and ProteinPhrophet algorithms (Keller *et al*, 2005; version 4.0) for the identification of peptides and proteins, respectively. In all the datasets presented the false discovery rate (FDR) was maintained below 1%. This was calculated based on the number of the decoy hits at the PeptideProphet cut-off score used.

Label-free quantification

For label-free quantification of the identified peptides, mzXML files were processed with OpenMS suite (Sturm *et al*, 2008; version 1.8) to detect and extract ion signals. Each signal feature was matched with the best peptide assignment obtained after database searching. Intensity maps were generated and aligned together with the corresponding peptide sequences. The results were exported to excel for further analysis.

Post-identification statistical analysis

Intensities of phospho-peptide signals were obtained by pairwise sample comparison, and the intensities of triplicate samples were averaged and normalized to the maximum intensity during the time course to obtain each peptide's profile. Further classification was performed as follows. Peptides were *included* and classified as disappearing when two sequential low values (defined as less than 40% of the first maximum value) were found. Peptides were classified as *early* when the first low value occurred at 20 min or less, as *late* when it occurred at 75 min or more, and as *intermediate* when it occurred in between these times. Peptides were *excluded* from this classification when (1) the first reduced value was less than 40% of the first maximum value; or (2) the first reduced value was less than 60% of the t=0 value; or (specifically for classification into the early category; (3)) the t=0 value was less than 50% of the maximum value. Peptides that did not pass the inclusion and/or exclusion filters were categorised either as *stable* (when fewer than 3 non-consecutive low values were observed during the time course), or alternatively as *rest*.

To assign protein stability, based on the results from the shotgun mass spectrometric survey, we considered a protein stable when more than half of the peptides corresponding to a protein fell into the *stable* category.

For analysis of dephosphorylation timing clustering, clustering scores were calculated amongst all phospho-peptides corresponding to one protein. For each protein, the numbers of peptides that did or did not co-occur in the same category were counted. These were summed for all relevant proteins, and the

clustering score was calculated as the number of co-occurrences expressed as a fraction of the number of all (co- and non-co-)occurrences. The clustering score was compared to the average of all empirical clustering scores in 2000 random simulations. In these simulations, the timing category occupancies were maintained. From sets of phospho-peptides differing only in charge, one was randomly picked to include only unique peptides in this analysis.

Two-tailed Fisher's exact tests were used for calculating p-values in all other enrichment analyses.

Release dates for genomic data were 13-05-2011 for the Saccharomyces Genome Database (SGD) Cdc14 physical interactor set; 13-05-2011 for AmiGO gene ontology classes; and 13-09-2013 for DAVID.

Yeast strains used in this study

Figure	Strain	Genotype
1/S1	Y141	*MATa ade2-1, trp1-1, can1-100, leu2-3,112, his3-11,15, ura3, GAL, psi+* (wild-type)
	Y4536	*MATa cdc14-3, trp1::TRP1-CDC14pr-CDC14-eGFP*
	Y4537	*MATa cdc14-3, trp1::TRP1-CDC14pr-CDC14-NLS-eGFP*
	Y151	*MATa cdc14-3*
2/S2	Y4536	*MATa cdc14-3, trp1::TRP1-CDC14pr-CDC14-eGFP*
	Y4537	*MATa cdc14-3, trp1::TRP1-CDC14pr-CDC14-NLS-eGFP*
	Y4538	*MATa cdc14-3, trp1::TRP1-CDC14pr-CDC14, his3::HIS3-TEF1pr-eGFP-SPO20(51-91)*
	Y4539	*MATa cdc14-3, trp1::TRP1-CDC14pr-CDC14-NLS, his3::HIS3-TEF1pr-eGFP-SPO20(51-91)*
	Y4540	*MATa cdc14-3, trp1::TRP1-CDC14pr-CDC14, his3::HIS3-SPC42-eYFP, HOF1-eGFP::LEU2*
	Y4541	*MATa cdc14-3, trp1::TRP1-CDC14pr-CDC14-NLS, his3::HIS3-SPC42-eYFP, HOF1-eGFP::LEU2*
	Y4542	*MATa cdc14-3, trp1::TRP1-CDC14pr-CDC14, his3::HIS3-SPC42-eYFP, INN1-eGFP::LEU2*
	Y4543	*MATa cdc14-3, trp1::TRP1-CDC14pr-CDC14-NLS, his3::HIS3-SPC42-eYFP, INN1-eGFP::LEU2*
	Y4544	*MATa cdc14-3, trp1::TRP1-CDC14pr-CDC14, his3::HIS3-SPC42-eYFP, CYK3-eGFP::LEU2*
	Y4545	*MATa cdc14-3, trp1::TRP1-CDC14pr-CDC14-NLS, his3::HIS3-SPC42-eYFP, CYK3-eGFP::LEU2*
	Y4546	*MATa cdc14-3, trp1::TRP1-CDC14pr-CDC14, his3::HIS3-SPC42-eYFP, MYO1-eGFP::LEU2*
	Y4547	*MATa cdc14-3, trp1::TRP1-CDC14pr-CDC14-NLS, his3::HIS3-SPC42-eYFP, MYO1-eGFP::LEU2*
	Y141	*MATa ade2-1, trp1-1, can1-100, leu2-3,112, his3-11,15, ura3, GAL, psi+* (wild-type)
	Y151	*MATa cdc14-3*
	Y4636	*MATa cdc14-1, trp1::TRP1-CDC14pr-CDC14-eGFP*
	Y4637	*MATa cdc14-1, trp1::TRP1-CDC14pr-CDC14-NLS-eGFP*
	Y4548	*MATa hof1Δ::HIS3*
	Y4549	*MATa cyk3Δ::HIS3*
	Y4550	*MATa cdc14-3, trp1::TRP1-CDC14pr-CDC14*
	Y4551	*MATa cdc14-3, trp1::TRP1-CDC14pr-CDC14-NLS*
	Y4552	*MATa cdc14-3, trp1::TRP1-CDC14pr-CDC14, hof1Δ::HIS3*
	Y4553	*MATa cdc14-3, trp1::TRP1-CDC14pr-CDC14-NLS, hof1Δ::HIS3*
	Y4554	*MATa cdc14-3, trp1::TRP1-CDC14pr-CDC14, cyk3Δ::HIS3*
	Y4555	*MATa cdc14-3, trp1::TRP1-CDC14pr-CDC14-NLS, cyk3Δ::HIS3*
3	Y4558	*MATα CDC20prΔ::TRP1-MET3pr::HA3, CDC14-HA6::HIS3, cdc15-as1::URA3*
	Y4559	*MATα CDC20prΔ::TRP1-MET3pr::HA3, ura3::URA3-GAL-SIC1-HA1, CDC14-HA6::HIS3, cdc15-as1::URA3*
	Y4560	*MATa CDC20prΔ::TRP1-MET3pr::HA3, his3::HIS3-GAL-CDC14-Pk, CDC14-*

		HA6::HIS3, cdc15-as1::URA3
	Y4561	*MATα CDC20prΔ::TRP1-MET3pr::HA3, ura3::URA3-GAL-SIC1-HA1, his3::HIS3-GAL-CDC14-Pk, CDC14-HA6::HIS3, cdc15-as1::URA3*
	Y403	*MATa CDC20prΔ::TRP1-MET3pr::HA3*
	Y4562	*MATa CDC20prΔ::TRP1-MET3pr::HA3, his3::HIS3-GAL-CDC14-Pk*
5*†/S4*†	Y4563	*MATa trp1::TRP1-CRE-EBD78, INN1::URA3-I30-CLB2m*
	Y4564	*MATa trp1::TRP1-CRE-EBD78, INN1::URA3-I30-CLB2mΔCDK*
	Y4565	*MATa trp1::TRP1-CRE-EBD78*
	Y4566	*MATa trp1::TRP1-CRE-EBD78, BNR1::URA3-I30-CLB2m*
	Y4567	*MATa trp1::TRP1-CRE-EBD78, BNR1::URA3-I30-CLB2mΔCDK*
	Y4568	*MATa trp1::TRP1-CRE-EBD78, CHS2::URA3-I30-CLB2m*
	Y4569	*MATa trp1::TRP1-CRE-EBD78, CHS2::URA3-I30-CLB2mΔCDK*
	Y4570	*MATa trp1::TRP1-CRE-EBD78, EDE1::URA3-I30-CLB2m*
	Y4571	*MATa trp1::TRP1-CRE-EBD78, EDE1::URA3-I30-CLB2mΔCDK*
	Y4572	*MATa trp1::TRP1-CRE-EBD78, AIP1::URA3-I30-CLB2m*
	Y4573	*MATa trp1::TRP1-CRE-EBD78, AIP1::URA3-I30-CLB2mΔCDK*
	Y4574	*MATa trp1::TRP1-CRE-EBD78, SRV2::URA3-I30-CLB2m*
	Y4575	*MATa trp1::TRP1-CRE-EBD78, SRV2::URA3-I30-CLB2mΔCDK*
	Y4576	*MATa his3::HIS3-TEF1pr-eGFP-SPO20(51-91)*
	Y4577	*MATa trp1::TRP1-CRE-EBD78, INN1::URA3-I30-CLB2m, his3::HIS3-TEF1pr-eGFP-SPO20(51-91)*
	Y4578	*MATa trp1::TRP1-CRE-EBD78, INN1::URA3-I30-CLB2mΔCDK, his3::HIS3-TEF1pr-eGFP-SPO20(51-91)*
	Y4579	*MATa trp1::TRP1-CRE-EBD78, CHS2::URA3-I30-CLB2m, his3::HIS3-TEF1pr-eGFP-SPO20(51-91)*
	Y4580	*MATa trp1::TRP1-CRE-EBD78, CHS2::URA3-I30-CLB2mΔCDK, his3::HIS3-TEF1pr-eGFP-SPO20(51-91)*
	Y4581	*MATa trp1::TRP1-CRE-EBD78, EDE1::URA3-I30-CLB2m, his3::HIS3-TEF1pr-eGFP-SPO20(51-91)*
	Y4582	*MATa trp1::TRP1-CRE-EBD78, EDE1::URA3-I30-CLB2mΔCDK, his3::HIS3-TEF1pr-eGFP-SPO20(51-91)*
	Y4583	*MATa trp1::TRP1-CRE-EBD78, AIP1::URA3-I30-CLB2m, his3::HIS3-TEF1pr-eGFP-SPO20(51-91)*
	Y4584	*MATa trp1::TRP1-CRE-EBD78, AIP1::URA3-I30-CLB2mΔCDK, his3::HIS3-TEF1pr-eGFP-SPO20(51-91)*
	Y4585	*MATa trp1::TRP1-CRE-EBD78, SRV2::URA3-I30-CLB2m, his3::HIS3-TEF1pr-eGFP-SPO20(51-91)*
	Y4586	*MATa trp1::TRP1-CRE-EBD78, SRV2::URA3-I30-CLB2mΔCDK, his3::HIS3-TEF1pr-eGFP-SPO20(51-91)*
	Y4587	*MATa trp1::TRP1-CRE-EBD78, SIC1::URA3-I10-CLB2m*
	Y4588	*MATa trp1::TRP1-CRE-EBD78, SIC1::URA3-I10-CLB2mΔCDK*
	Y4589	*MATa trp1::TRP1-CRE-EBD78, SIC1::URA3-I30-CLB2m*
	Y4590	*MATa trp1::TRP1-CRE-EBD78, SIC1::URA3-I30-CLB2mΔCDK*
	Y4591	*MATa trp1::TRP1-CRE-EBD78, INN1::URA3-I10-CLB2m*
	Y4592	*MATa trp1::TRP1-CRE-EBD78, INN1::URA3-I10-CLB2mΔCDK*

	Y4593	*MATa trp1::TRP1-CRE-EBD78, ASK1::URA3-l30-CLB2m*
	Y4594	*MATa trp1::TRP1-CRE-EBD78, ASK1::URA3-l30-CLB2mΔCDK*
6*/S4*	Y4565	*MATa trp1::TRP1-CRE-EBD78*
	Y4595	*MATa trp1::TRP1-CRE-EBD78, INN1::INN1::URA3-l30-CLB2m*
	Y4596	*MATa trp1::TRP1-CRE-EBD78, INN1::inn1(5A)::URA3-l30-CLB2m*
	Y4597	*MATa trp1::TRP1-CRE-EBD78, INN1::INN1::URA3-l30-CLB2mΔCDK*
	Y4598	*MATa trp1::TRP1-CRE-EBD78, INN1::inn1(5A)::URA3-l30-CLB2mΔCDK*
	Y4599	*MATa trp1::TRP1-CRE-EBD78, EDE1::EDE1::URA3-l30-CLB2m*
	Y4600	*MATa trp1::TRP1-CRE-EBD78, EDE1::ede1(15A)::URA3-l30-CLB2m*
	Y4601	*MATa trp1::TRP1-CRE-EBD78, EDE1::EDE1::URA3-l30-CLB2mΔCDK*
	Y4602	*MATa trp1::TRP1-CRE-EBD78, EDE1::ede1(15A)::URA3-l30-CLB2mΔCDK*
	Y4603	*MATa trp1::TRP1-CRE-EBD78, AIP1::AIP1::URA3-l30-CLB2m*
	Y4604	*MATa trp1::TRP1-CRE-EBD78, AIP1::aip1(6A)::URA3-l30-CLB2m*
	Y4605	*MATa trp1::TRP1-CRE-EBD78, AIP1::AIP1::URA3-l30-CLB2mΔCDK*
	Y4606	*MATa trp1::TRP1-CRE-EBD78, AIP1::aip1(6A)::URA3-l30-CLB2mΔCDK*
	Y4607	*MATa trp1::TRP1-CRE-EBD78, SRV2::SRV2::URA3-l30-CLB2m*
	Y4608	*MATa trp1::TRP1-CRE-EBD78, SRV2::srv2(4A)::URA3-l30-CLB2m*
	Y4609	*MATa trp1::TRP1-CRE-EBD78, SRV2::SRV2::URA3-l30-CLB2mΔCDK*
	Y4610	*MATa trp1::TRP1-CRE-EBD78, SRV2::srv2(4A)::URA3-l30-CLB2mΔCDK*
	Y4611	*MATa trp1::TRP1-CRE-EBD78, INN1::INN1::URA3-l30-CLB2m, his3::HIS3-TEF1pr-eGFP-SPO20(51-91)*
	Y4612	*MATa trp1::TRP1-CRE-EBD78, INN1::inn1(5A)::URA3-l30-CLB2m, his3::HIS3-TEF1pr-eGFP-SPO20(51-91)*
	Y4613	*MATa trp1::TRP1-CRE-EBD78, INN1::INN1::URA3-l30-CLB2mΔCDK, his3::HIS3-TEF1pr-eGFP-SPO20(51-91)*
	Y4614	*MATa trp1::TRP1-CRE-EBD78, INN1::inn1(5A)::URA3-l30-CLB2mΔCDK, his3::HIS3-TEF1pr-eGFP-SPO20(51-91)*
	Y4615	*MATa trp1::TRP1-CRE-EBD78, EDE1::EDE1::URA3-l30-CLB2m, his3::HIS3-TEF1pr-eGFP-SPO20(51-91)*
	Y4616	*MATa trp1::TRP1-CRE-EBD78, EDE1::ede1(15A)::URA3-l30-CLB2m, his3::HIS3-TEF1pr-eGFP-SPO20(51-91)*
	Y4617	*MATa trp1::TRP1-CRE-EBD78, EDE1::EDE1::URA3-l30-CLB2mΔCDK, his3::HIS3-TEF1pr-eGFP-SPO20(51-91)*
	Y4618	*MATa trp1::TRP1-CRE-EBD78, EDE1::ede1(15A)::URA3-l30-CLB2mΔCDK, his3::HIS3-TEF1pr-eGFP-SPO20(51-91)*
	Y4619	*MATa trp1::TRP1-CRE-EBD78, AIP1::AIP1::URA3-l30-CLB2m, his3::HIS3-TEF1pr-eGFP-SPO20(51-91)*
	Y4620	*MATa trp1::TRP1-CRE-EBD78, AIP1::aip1(6A)::URA3-l30-CLB2m, his3::HIS3-TEF1pr-eGFP-SPO20(51-91)*
	Y4621	*MATa trp1::TRP1-CRE-EBD78, AIP1::AIP1::URA3-l30-CLB2mΔCDK, his3::HIS3-TEF1pr-eGFP-SPO20(51-91)*
	Y4622	*MATa trp1::TRP1-CRE-EBD78, AIP1::aip1(6A)::URA3-l30-CLB2mΔCDK, his3::HIS3-TEF1pr-eGFP-SPO20(51-91)*

	Y141	*MATa ade2-1, trp1-1, can1-100, leu2-3,112, his3-11,15, ura3, GAL, psi+* (wild-type)
	Y4685	*MATa ede1Δ::LEU2*
	Y4687	*MATa aip1Δ::TRP1*
	Y4695	*MATa INN1::INN1-aid::KAN pADH1-OsTir1-9Myc::ADE2*
	Y4690	*MATa INN1::INN1-aid::KAN pADH1-OsTir1-9Myc::ADE2 ede1Δ::LEU2*
	Y4689	*MATa INN1::INN1-aid::KAN pADH1-OsTir1-9Myc::ADE2 aip1Δ::TRP1*
	Y4548	*MATa hof1Δ::HIS3*
	Y4697	*MATa ede1Δ::LEU2 hof1Δ::HIS3*
	Y4696	*MATa aip1Δ::TRP1 hof1Δ::HIS3*
7/S5*	Y4623	*MATa trp1::TRP1-CRE-EBD78, INN1::URA3-l30-CLB2m, his3::HIS3-SPC42-eYFP, CHS2-eGFP::LEU2*
	Y4624	*MATa trp1::TRP1-CRE-EBD78, INN1::URA3-l30-CLB2mΔCDK, his3::HIS3-SPC42-eYFP, CHS2-eGFP::LEU2*
	Y4625	*MATa trp1::TRP1-CRE-EBD78, INN1::URA3-l30-CLB2m, his3::HIS3-SPC42-eYFP, CYK3-eGFP::LEU2*
	Y4626	*MATa trp1::TRP1-CRE-EBD78, INN1::URA3-l30-CLB2mΔCDK, his3::HIS3-SPC42-eYFP, CYK3-eGFP::LEU2*
	Y4563	*MATa trp1::TRP1-CRE-EBD78, INN1::URA3-l30-CLB2m*
	Y4564	*MATa trp1::TRP1-CRE-EBD78, INN1::URA3-l30-CLB2mΔCDK*
	Y4627	*MATa trp1::TRP1-CRE-EBD78, INN1::URA3-l30-CLB2m-eGFP, his3::HIS3-SPC42-eYFP*
	Y4628	*MATa trp1::TRP1-CRE-EBD78, INN1::URA3-l30-CLB2mΔCDK-eGFP, his3::HIS3-SPC42-eYFP*
	Y4629	*MATa trp1::TRP1-CRE-EBD78, INN1::URA3-l30-CLB2m, his3::HIS3-SPC42-eYFP, MYO1-eGFP::LEU2*
	Y4630	*MATa trp1::TRP1-CRE-EBD78, INN1::URA3-l30-CLB2mΔCDK, his3::HIS3-SPC42-eYFP, MYO1-eGFP::LEU2*
	Y4699	*MATa trp1::TRP1-CRE-EBD78, INN1::inn1(5A)::URA3-l30-CLB2m, his3::HIS3-SPC42-eYFP, MYO1-eGFP::LEU2*
	Y4700	*MATa trp1::TRP1-CRE-EBD78, INN1::inn1(5A)::URA3-l30-CLB2mΔCDK, his3::HIS3-SPC42-eYFP, MYO1-eGFP::LEU2*
	Y4631	*MATa trp1::TRP1-CRE-EBD78, INN1::URA3-l30-CLB2m, pRS313-CHS2pr-CHS2(V377I)-HIS3*
	Y4632	*MATa trp1::TRP1-CRE-EBD78, INN1::URA3-l30-CLB2mΔCDK, pRS313-CHS2pr-CHS2(V377I)-HIS3*
	Y4577	*MATa trp1::TRP1-CRE-EBD78, INN1::URA3-l30-CLB2m, his3::HIS3-TEF1pr-eGFP-SPO20(51-91)*
	Y4578	*MATa trp1::TRP1-CRE-EBD78, INN1::URA3-l30-CLB2mΔCDK, his3::HIS3-TEF1pr-eGFP-SPO20(51-91)*
	Y4633	*MATa trp1::TRP1-CRE-EBD78, CHS2::URA3-l30-CLB2m, his3::HIS3-TEF1pr-eGFP-SPO20(51-91)*
	Y4634	*MATa trp1::TRP1-CRE-EBD78, CHS2::URA3-l30-CLB2mΔCDK, his3::HIS3-TEF1pr-eGFP-SPO20(51-91)*

* l10 and l30 refer to *LoxP-HA3-URA3-LoxP-Linker* conditional fusion cassettes with linker lengths of 10 and 30 amino acids, respectively. *CLB2m* refers to the *CLB2ΔDBΔken1,2ΔNLS* mutant used for

conditional cyclin fusion. See also Figure 5A and Materials and Methods.

† Strains for screening other candidates that are not listed here, were similarly created.

Supplementary References

Bodenmiller B & Aebersold R (2010) Quantitative analysis of protein phosphorylation on a system-wide scale by mass spectrometry-based proteomics. *Meth. Enzymol.* **470:** 317–334

Keller A, Eng J, Zhang N, Li X-J & Aebersold R (2005) A uniform proteomics MS/MS analysis platform utilizing open XML file formats. *Mol. Syst. Biol.* **1:** 2005.0017

Moseley JB & Goode BL (2006) The yeast actin cytoskeleton: from cellular function to biochemical mechanism. *Microbiol. Mol. Biol. Rev.* **70:** 605–645

Sturm M, Bertsch A, Gröpl C, Hildebrandt A, Hussong R, Lange E, Pfeifer N, Schulz-Trieglaff O, Zerck A, Reinert K & Kohlbacher O (2008) OpenMS - an open-source software framework for mass spectrometry. *BMC Bioinformatics* **9:** 163

Verma R, Annan RS, Huddleston MJ, Carr SA, Reynard G & Deshaies RJ (1997) Phosphorylation of Sic1p by G1 Cdk required for its degradation and entry into S phase. *Science* **278:** 455–460